ORIGINAL ARTICLE

CrossMark

Kinetic analysis of hydrocarbon generation based on saline lacustrine source rock and kerogen samples in the western Qaidam Basin, China

Li Xu[1] · Yajun Shi[1] · Xiaodong Chen[2] · Chuanzhi Wan[1] · Jiangong Wang[1]

Abstract

Tertiary carbonate rocks from the Qaidam Basin in China are typical plateau saline lacustrine source rocks. Despite the fact that this set of source rocks has a relatively low abundance of organic matter (major frequency of total organic carbon, 0.4–0.6%), the organic matter has a high hydrocarbon conversion rate and commonly forms low-maturity oil. In this study, a comparative analysis was conducted on Tertiary source rock and kerogen samples from the Qaidam Basin using a kinetic experiment of hydrocarbon generation. The objectives of the study were to investigate the mechanism of hydrocarbon generation from source rock to low-maturity oil and the catalysis of kerogen pyrolysis by minerals. The results showed that both the source rock and kerogen samples reached a maximum liquid hydrocarbon yield during the low-maturity stage. Eighty percent of the hydrocarbons were expulsed before the Easy Ro reached 0.8%. Special algal parent materials in the saline lacustrine basin could be the primary cause that leads to generating low-maturity oil. Compared to the kerogen samples, the source rock was more prone to hydrocarbon generation via pyrolysis. The latter had a higher liquid hydrocarbon yield per unit organic matter and a lower activation energy; thus, it entered the hydrocarbon generation threshold earlier. The key factor for the aforementioned differences might be catalysis by minerals (particularly carbonate minerals) and the presence of soluble organic matter in the source rocks.

Keywords Pyrolysis · Kinetics · Source rocks · Kerogen · Saline lacustrine basin

Introduction

Based on thermal simulation experiments with rapid temperature ramping (Connan 1974; Waples 1981), numerous studies have investigated the hydrocarbon generation mechanism and the evolution pattern of source rocks. In addition to the widely accepted theory of oil generation by the pyrolysis of kerogen (Tissot and Espitalié 1975), hydrocarbon generation from source rocks is affected by multiple factors. For example, minerals have a certain catalytic effect in the generation of oil and gas, particularly clay minerals and carbonate minerals (Tannenbaum and Kaplan 1985; Bagri and Williams 2002; Saxby et al. 1992; Pan et al. 2010; Zhang et al. 2005). Different types of clay minerals have varying catalytic effects on hydrocarbon generation from organic matter, ranking from high to low in the order of illite, kaolinite, and montmorillonite. Among these minerals, illite shows the most prominent catalytic effect, which can increase the amount of hydrocarbon generation by approximately 17.5% (Li et al. 2002). Brooks (1948) found that acidified clays catalyze the isomerization. Montmorillonite, illite, and kaolinite increase the light hydrocarbon contents and decrease the heavy hydrocarbon contents in the pyrolysis of saturated hydrocarbons (Mackenzie et al. 1983). Carbonate minerals in terrestrial carbonate rocks as source rocks for hydrocarbons alter the composition of kerogen pyrolysis products and improve the total hydrocarbon generation (Xie et al. 2000; Li et al. 2002; Wang et al. 2009; Ma et al. 2013; Saxby et al. 1992; Pan et al. 2010). Prior results have demonstrated that minerals have a significant catalytic effect on hydrocarbon generation from terrestrial source rocks, particularly terrestrial saline lacustrine basins containing high levels of carbonate minerals. However, due to the complexity of geological conditions in terrestrial saline lacustrine basins, there is

✉ Li Xu
  xuli0055@126.com

[1] Petrochina Research Institute of Petroleum Exploration and Development-Northwest, 730020 Lanzhou, Gansu, China

[2] Qinghai Oilfield Research Institute of Exploration, 736206 Dunhuang, Gansu, China

controversy over the catalytic hydrocarbon generation from sedimentary organic matter. Previous hydrocarbon generation simulations have shown that the comparative analysis of source rocks and kerogen samples in a specific basin can more effectively reflect the hydrocarbon generation process and the hydrocarbon generation potential of organic matter. Additionally, it has spurred investigations into the impact of mineral composition on the catalysis of kerogen pyrolysis and the kinetic parameters of hydrocarbon generation (Reynolds and Burnham 1995; Lewan et al. 1979; Bechar et al. 1992; Seewald et al. 1998; Tang et al. 2014).

Tertiary source rocks in the Qaidam Basin are typical plateau saline lacustrine source rocks (Huang et al. 2016; Peng 2005). This set of source rocks commonly has a low maturity with an Ro of 0.5–0.9% (23 samples) and 82% of the samples are characterized by $T_{max} < 435$ °C (86 samples). The parent materials for hydrocarbon generation are primarily aquatic organisms with a large contribution from algae (Zhou et al. 2002) and a limited input from terrestrial higher plants (Hanson et al. 2001).There are primarily organic matter types I–II1. The total organic carbon (TOC) content of effective source rocks ranges between 0.4 and 2.66% (135 samples), with a mean content of 0.81%. The TOC content is between 0.4 and 0.6% for 48% of the samples, with an overall low abundance of organic matter. However, this set of source rocks has a high hydrocarbon conversion rate. The chloroform "A"/TOC is generally 20% and up to 60% or greater. The total hydrocarbon/TOC is generally 12% and up to 40% or greater (Peng 2005). The yield of liquid hydrocarbons per unit organic matter is generally higher than that of source rocks from saline lacustrine basins in East China. In the present study, a comparative analysis was conducted on Tertiary source rocks and their kerogen from the Qaidam Basin using a gold tube-autoclave closed system for thermal simulation experiments. The mechanism of hydrocarbon generation from source rocks to low-mature oil and the catalysis of kerogen pyrolysis by minerals are discussed. Furthermore, the hydrocarbon generation history in the study area was further clarified by a comparison with actual geological conditions.

In the present study, samples were collected from the Hongshi depression of the western Qaidam Basin. This depression is located in the Shizigou area at the western piedmont of the Altun Mountains in the southwestern Qaidam Basin. It is the main hydrocarbon generation center that has been found relatively early and reliably studied in the Qaidam Basin, covering an area of 326 km². This depression belongs to the persistent-subsidence type and has characteristics of superimposition of multiple sets of source rocks. According to statistics, the thickness of dark mudstone ranges from 800 to 1410 m, wherein the E_3^2 are the major source rocks with a wide range of distribution and high hydrocarbon generation capacity. For the total

source rocks, the gammacerane to C_{30}-hopaneratio and the C_{35}-hopane to C_{34}-hopane ratios are greater than 1, which show a high-salinity, highly reduced sedimentary environment and represent typical saline lacustrine source rocks in the Qaidam Basin.

Geological and geochemical settings

The Qaidam Basin is located in the northeastern Tibetan Plateau, China (Fig. 1). This basin borders the East Kunlun Mountains to the south, the Qilian Mountains to the north, and the Altun Mountains to the west. The basin has a slightly triangular shape and covers an area of 12.1×10^4 km²(Guo et al. 2017). The Mesozoic–Cenozoic Qaidam Basin belongs to the giant basin system around the Tibetan Plateau. As influenced by the Himalayan movement, the basin overall experienced three tectonic evolutionary stages in the Mesozoic–Cenozoic period, i.e., the early stage of the Jurassic rift, the middle stage of Tertiary subsidence and depression, and the late stage of the Late Neogene–Quaternary uplift and inversion. The basin can be divided into three first-order tectonic units in the plane, i.e., the northern fault block, the western depression, and the eastern depression (Cao et al. 2014).

In the Qaidam Basin, more than 80% of the oil and gas are concentrated in the western region. This region has primarily developed a set of Tertiary plateau saline lacustrine sediments. The lower Ganchaigou Formation (E_3^2) and upper Ganchaigou Formation (N_1) consist of a set of deep-semideep lacustrine deposits, primarily comprising calcareous mudstone, gypsum-containing shale, and calcareous shale in an inter bedded or phase-transformation contact relationship with evaporates, such as marlstone, gypsum bed, and rock salt bed. These typical saline lacustrine source rocks were formed in a high salinity and strong reducing depositional environment. The phytane to pristane ratio (pr/ph) ranges from 0.2 to 0.4; the gammacerane to C_{30}-hopane ratio is greater than 1.

Samples and experiments

Samples

Samples for the thermal simulation were collected from the E_3^2 stratum in well Shi23 in the Hongshi depression of the western Qaidam Basin (Fig. 1). The sampling depth was 3990.1 m. The core samples were 2.5 cm in diameter and 5 cm in height (Fig. 2). The samples contained 0.86% TOC with a T_{MAX} of 418 °C and type II1 kerogen. The basic geochemical parameters of the samples are shown in Table 1. The sample has a relatively low abundance of organic matter
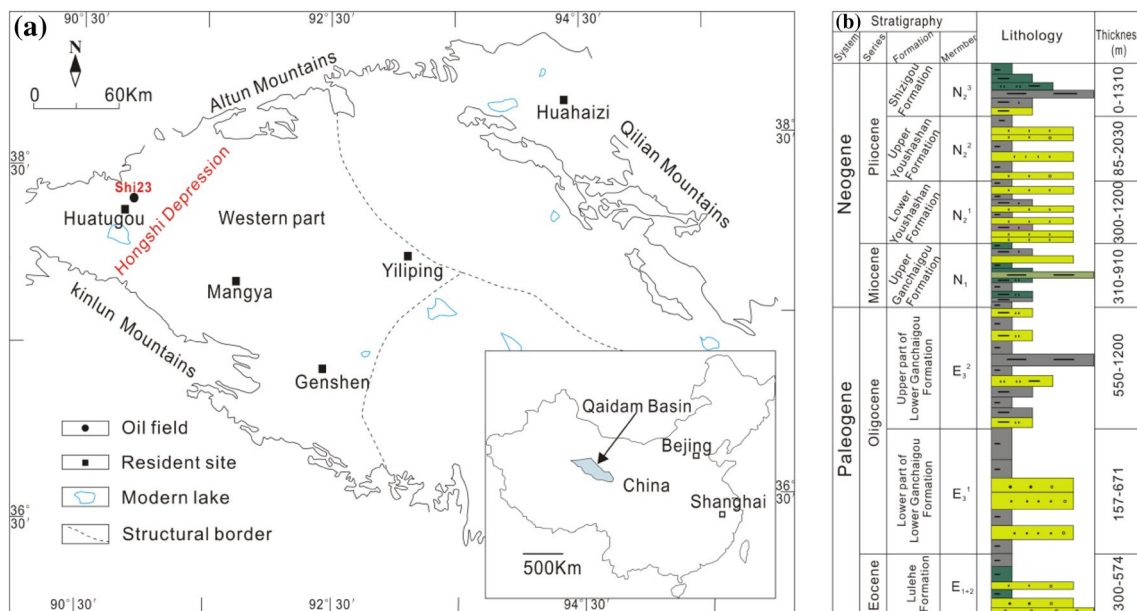
Fig. 1 Map showing the geographical position of tectonic units in the Qaidam Basin, China

Fig. 2 The pictures of the samples

(total organic carbon is 0.86%) and low maturity. Its HI is 562 mg/g.TOC, belonging to II2 organic matter. In the

whole-rock mineral composition of the samples, clay minerals were mainly illite and chlorite. Additionally, it contained 23.1% carbonate minerals, including 17.8% calcite and 5.3% dolomite (Table 2); the sample belongs to a typical Saline lacustrine source rock, which has a high carbonate content and pyrite. The source rock forms a strong reducing and high salt environment.

Geochemical data of source rocks were conducted using the Rock-eval6 pyrolysis equipment; the pictures of these equipments are shown in Fig. 3a. The mineral composition was analyzed using BRUKERD8ADVANCEX-ray diffraction (Germany). The diffract meter was operated at a voltage of 40 kV and a current of 30 mA. The samples were scanned in the range of $2\theta = 3$–$85°$ at a slit width of 1 mm and at a rate of 4 per min; the pictures of these equipments are shown in Fig. 3b.

The samples were cleaned and ground to 100 mesh before division into two portions. One portion was directly used

Table 1 Geochemical data of source rocks from well Shi23, Qaidam Basin, China

Sample	Stratum	Depth	TOC (%)	T_{max} (°C)	S1 (mg/g)	S2 (mg/g)	S3 (mg/g)	HI (mg/g.TOC)	OI (mg/g.TOC)	Kerogen type
Shi23	E_3^2	3990.1 m	0.86	418	2.13	4.83	1.40	562	163	II$_1$

Table 2 Mineral composition of source rocks from well Shi23, Qaidam Basin, China

Sample	Stratum	Mineral composition(%)						
		Quartz	Feldspar	Illite	Chlorite	Calcite	Dolomite	Pyrite
Shi23	E_3^2	13.1	26.1	20.5	14.3	17.8	5.3	3
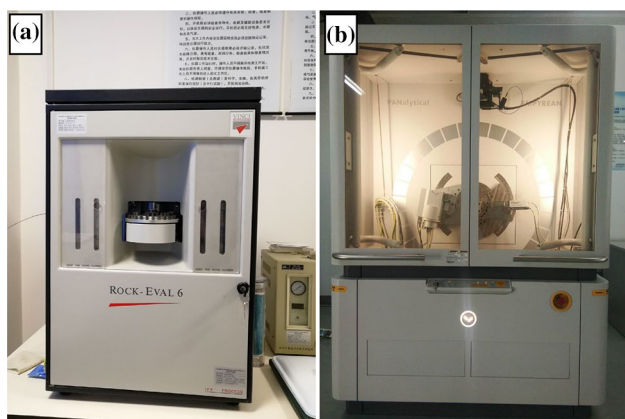
Fig. 3 The pictures of the equipments for the data (**a**: shown in Table 1; **b**: shown in Table 2)

Fig. 4 Sketch of the gold tube simulation system

as the source rocks sample for the thermal simulation (50 g in total, uniformly divided into 12 subsamples). The other portion (120 g) was thoroughly soaked in 6 mol/L hydrochloric acid until no bubbles occurred; the sample was then placed in a water bath (90 °C) and heated for 4 h for segregation, followed by three washes with deionized water; a 48% hydrofluoric acid solution was added in an acidic condition and allowed to react in the water bath for 4 h; the sample was washed, and the above procedures with hydrochloric acid and hydrofluoric acid solution were repeated three times; the sample was repeatedly washed with distilled water to neutral to completely remove carbonate and silicate materials in the source rock and then dried to prepare the kerogen. A total of 1.28 g of kerogen was obtained and uniformly divided into 12 subsamples.
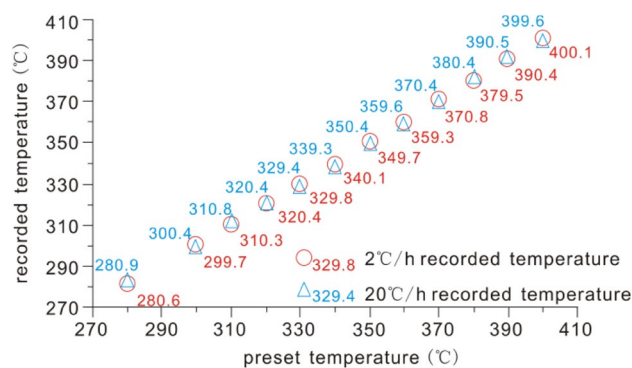
Pyrolysis

The pyrolytic simulation experiment was conducted in the State Key Laboratory of Organic Geochemistry, Guangzhou Institute of Geochemistry, Chinese Academy of Sciences. The experimental device was a gold tube-autoclave closed thermal simulation system. The device features and the experimental procedures are described in detail in the literature (Xiao et al. 2005; Li et al. 2013) and a sketch diagram of the equipment is shown in Fig. 4. The experimental procedure was as follows. An appropriate amount of the sample was loaded into a gold tube. After displacing the air in the tube with argon gas, the gold tube opening was sealed using an argon-arc welder. The gold tube was placed into a cold-seal autoclave with externally controlled pressure and the autoclave was then placed into a pyrolysis furnace with a program-controlled temperature. The temperature program and pressure were set to perform the experiment. The pressure gauge of the autoclave was turned off at every experimental temperature. The autoclave was removed
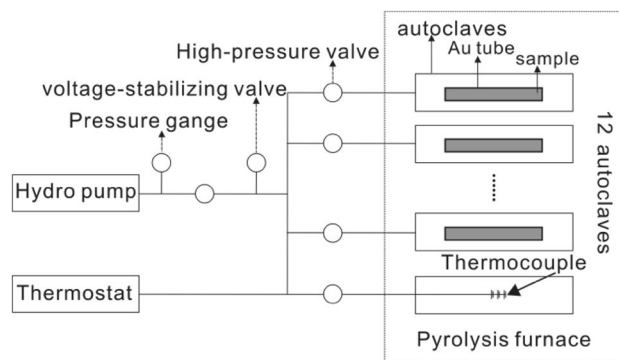
from the electronic furnace and quenched with cold water to room temperature. The pyrolysis products were extracted and quantified.

For comparison, the same temperature ramping program and pressure were used for the source rock and kerogen samples in the experiment. Moreover, the two groups of samples (source rock and kerogen) were used for pyrolytic simulation using two temperature ramping programs, slow at 2 °C/h and fast at 20 °C/h. First, the temperature was rapidly (1 h) increased to 200 °C and held for 2 h; then, the device was heated to 400 °C at ramping rates of 2 or 20 °C/h. The correlogram of preset temperature and recorded temperature in the pyrolysis experiment (Fig. 5) shows that the temperature error was less than 1 °C. Each group of samples was tested at 12 temperature points and removed at the target temperature. The pyrolysis products at varying temperatures were subjected to Soxhlet extraction using a ternary organic solvent (methanol: benzene: acetone, 2:1:1, v/v). Soluble organic matter was volatilized at room temperature and weighed to calculate the yield of liquid hydrocarbons. Based on the actual formation pressure in the study area, the pressure in this experiment was set to 50 MPa, while the actual pressure

Fig. 5 The correlogram of preset temperature and recorded temperature in the pyrolysis experiment

ranged from 49.6 to 50.3 MPa; the pressure error was less than 1 MPa.

Results and discussion

Hydrocarbon conversion

Formation and cracking of liquid hydrocarbons

Table 3 shows the liquid hydrocarbon yields from pyrolysis. At the same temperature ramping rates, the liquid hydrocarbon yields exhibited similar hydrocarbon generation patterns between the source rock and kerogen samples. The liquid hydrocarbon yields increased with increasing temperature and reached the hydrocarbon generation peak at the

Table 3 Pyrolysates of the source rock and kerogen samples at different temperatures and different ramping rates

Temperature (°C)	Easy RO (%)	Hydrocarbon conversion (mg/g.rock)		Hydrocarbon conversion (mg/g.TOC)	
		Source rock	Kerogen	Source rock	Kerogen
2 °C/h ramping rate					
280	0.47	0.52	40.63	60.59	56.98
300	0.55	1.073	101.65	201.49	142.57
310	0.60	2.73	136.87	318.01	191.97
320	0.66	3.85	165.07	447.26	231.51
330	0.70	5.08	187.41	590.93	262.85
340	0.75	5.93	198.57	690.04	278.50
350	0.80	4.09	153.88	475.81	215.83
360	0.86	2.22	104.32	258.05	146.31
370	0.94	0.68	70.68	78.93	99.14
380	1.04	0.52	56.62	60.06	79.41
390	1.14	0.53	56.30	61.74	78.97
400	1.26	0.48	64.49	55.48	90.45
20 °C/h ramping rate					
280	0.37	0.16	14.10	19.06	19.78
300	0.43	0.41	24.41	47.98	34.23
310	0.47	0.72	39.17	84.29	54.93
320	0.51	1.16	69.74	134.66	97.81
330	0.54	1.97	101.89	228.55	142.91
340	0.59	2.83	133.95	328.94	187.87
350	0.64	4.17	162.49	485.08	227.90
360	0.68	5.21	183.52	606.17	257.38
370	0.72	3.16	151.14	367.32	211.98
380	0.77	0.66	109.90	77.11	154.13
390	0.82	0.18	59.12	21.43	82.92
400	0.89	0.31	52.18	36.00	73.18

Hydrocarbon conversion (mg/g.rock) $= m_{\text{Soluble organic matter}} \cdot \text{mg} / m_{\text{sample}}$ g

Hydrocarbon conversion (mg/g.TOC) $= m_{\text{Soluble organic matter}} \cdot \text{mg} / (m_{\text{sample}} \times \text{TOC}_{\text{sample}})$ g

same temperature; thereafter, the liquid hydrocarbon yields declined due to the production of gaseous hydrocarbons and light oil from secondary hydrocarbon cracking. Different temperature ramping rates affected the temperature at which the maximum yield was achieved and the amount of hydrocarbons generated from the samples. For example, at the slow ramping rate (2 °C/h), the source rocks obtained a maximum yield at 340 °C and achieved a maximum hydrocarbon generation of 5.93 mg/g rock. At the fast ramping rate (20 °C/h), the source rock obtained a maximum yield at 360 °C and the maximum hydrocarbon generation was 5.21 mg/g rock. The results demonstrated that the hydrocarbon generation rate was higher and that the hydrocarbon generation peak occurred earlier at the slow ramping rate compared with that of the fast ramping rate. This result indicates a mutual compensation relationship between time and temperature in the hydrocarbon generation process.

Hydrocarbon generation stages

At the temperature ramping rates of 2 and 20 °C/h, the samples obtained a maximum yield of liquid hydrocarbons at 340 and 360 °C (Table 3), respectively. When using the same experimental device for the pyrolysis of freshwater lacustrine source rocks, Liu et al. (2016) found that the source rocks reached the maximum liquid hydrocarbon yield at 380 and 430 °C, respectively. The samples from our study area exhibited the characteristics of hydrocarbon generation at lower temperatures compared with that of the freshwater lacustrine source rocks. Here, we used the model proposed by Sweeney and Burnham (1990) to convert the pyrolysis temperature into the Easy Ro data to obtain the relationship between the liquid hydrocarbon yield and Easy Ro. At the ramping rate of 2 °C/h, the source rocks reached a maximum hydrocarbon generation rate at an Easy Ro of 0.75, and 80% of the hydrocarbons were expulsed before the Easy Ro reached 0.8%. The samples obtained a maximum liquid hydrocarbon yield at the low-mature stage. This differed from the other kerogen samples that commonly showed their peak of liquid hydrocarbon yield at an Ro of approximately 1.0%.

Both the source rock and kerogen samples generated a large amount of hydrocarbons in the low-mature stage. This suggests that minerals contained in the source rocks had no significant catalytic effect on oil generation from hydrocarbons in the low-mature stage. The occurrence of large-scale hydrocarbon generation from organic matter in the low-mature stage might be related to the special saline lacustrine algal parent materials for hydrocarbon generation. For source rocks of different organic matter types, there are often large differences in terms of hydrocarbon generation potential and activation energy (Tissot et al. 1987; Huang et al. 1984). For better organic matter, the hydrocarbon generation

potential is higher, whereas the activation energy of source rocks is lower (Tissot et al. 1987; Huang et al. 1984; Fu and Shi 1975), allowing the hydrocarbon generation threshold to be reached earlier (Jiang et al. 2010). A study has shown that the parent materials for hydrocarbon generation from Tertiary source rocks in the Qaidam Basin are primarily *Botryococcus braunii* and *coccolithophores*(Zhou et al. 2002). A thermal simulation found that *coccolithophores* commonly generate a large amount of hydrocarbons during the low-mature stage (Song and Li 1995).

Hydrocarbon generation potential

The liquid hydrocarbon yields per unit organic matter significantly differed between the source rock and kerogen samples (Fig. 6). For example, in the experiment at the slow temperature ramping rate (2 °C/h), the source rock produced slightly higher liquid hydrocarbon yields compared with the kerogen samples in the temperature range of 280–320 °C. The liquid hydrocarbon yields of the source rocks rapidly increased and were significantly higher than those of the kerogen samples in the temperature range of 320–340 °C. The largest gap between the two groups was found at 340 °C, i.e., 690.04 mg/g.TOC for the source rocks and 278.50 mg/g. TOC for the kerogen samples. In the temperature range of 340–370 °C, the liquid hydrocarbon yields were lower for both groups. The source rock value sharply declined, but remained slightly higher than those of the kerogen samples. In the temperature range of 370–400 °C, the decline in

liquid hydrocarbon yields slowed down and the value was lower for the source rocks compared with that of the kerogen. Overall, the liquid hydrocarbon yields of the source rock were much higher than those of the kerogen. Tang et al. (2014) pyrolyzed source rock and kerogen samples from the Pearl River Estuary Basin and found that the hydrocarbon gas yield per unit organic matter was higher for the source rocks compared with the kerogen samples. This is similar to our experimental result in the present study. The source rock had higher liquid hydrocarbon yields than the kerogen, which is perhaps due to the catalytic effect of minerals and the presence of certain soluble organic matter (Rock-eval analysis: $S_1 = 2.13$ mg/g.rock) in the source rock.

Kinetic parameters

Discrete analysis of the accumulated hydrocarbon generation yield from the simulation samples at different temperature ramping rates allows for the fitting of the kinetic equation and solving the kinetic parameters for hydrocarbon generation from the source rock and kerogen samples (Liu and Tang 1998). Here, the kinetic parameters were calculated and the experimental results were simulated using Kinetics 2000. After the fitting calculation, we obtained the fitting curves for the conversion rate of liquid hydrocarbons produced via pyrolysis of the source rock and kerogen samples (Fig. 7). The curves showed a high fitting degree and the fitting results of the kinetic parameters were generally accurate.

Fig. 6 Hydrocarbon conversion for the source rock and kerogen samples. (**a**: at a ramping rate of 2 °C/h; **b**: at a ramping rate of 20 °C/h)
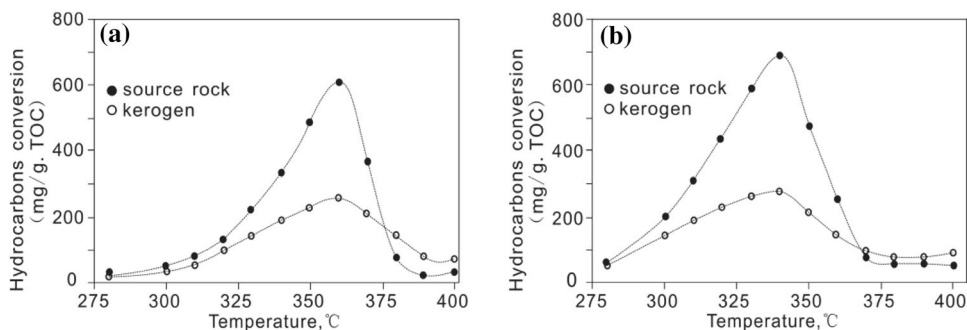
Fig. 7 Experimental and calculated conversion of pyrolysates at ramping rates of 2 and 20 °C/h, respectively(**a**: kerogen; **b**: source rock)
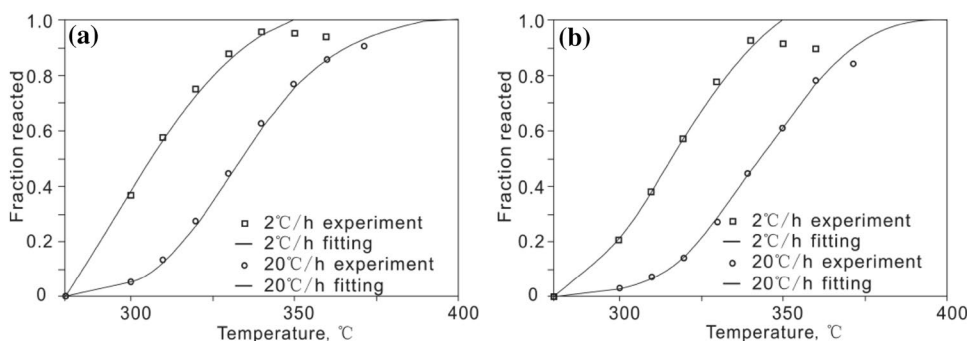
The pre-exponential factor was fixed at $A = 9.9970E + 15$ s^{-1} by multiple fittings. The activation energy of various group components in liquid hydrocarbons produced via pyrolysis of the source rock and kerogen samples generally showed similar distributions in the range of 52–58 kcal/mol (Fig. 8). Behar et al. (2010) reported that the activation energy of type I kerogen is distributed between 48 and 66 kcal/mol; the mean activation energy is 56 kcal/mol and the corresponding pre-exponential factor is $A = 5.64E + 14$ s^{-1}. Thus, our results were close to those of the previous study.

However, the major frequency peak of activation energy differed between the source rock and kerogen samples. The major frequency of activation energy for the source rocks was 53 kcal/mol, and that for the kerogen was 55 kcal/mol. According to an estimation by the empirical Arrhenius formula ($K = Ae^{-Ea/RT}$), if the activation energy is lowered by 10 kJ/mol, the reaction rate will increase by 50 times. Thus, the source rock with relatively low activation energy is more prone to hydrocarbon generation via pyrolysis compared to kerogen. Catalysis of organic matter pyrolysis for hydrocarbon generation by inorganic minerals in the source rocks was the primary cause leading to the decreased activation energy.

Geological applications

Hydrocarbon generation history

The hydrogen expulsion time of organic matter can be accurately deduced using the kinetic parameters of hydrogen generation (activation energy and pre-exponential factor) in combination with the thermal evolutionary history of the basin (Guo et al. 2009). In the present study, the thermal simulation samples were taken from the Hongshi depression, a major hydrocarbon-generating depression in the western Qaidam Basin. The Hongshi depression is located in the western section in the piedmont of the Altun Mountains with an area of 326 km^2, an ancient surface temperature of 14 °C, and an ancient geothermal gradient of 2.4 °C/100 m. The Hongshi depression continued to subside prior to late

Himalayan tectonic activity; then (4 Ma), it was strongly uplifted and was denudated (Fig. 9). The maximum denudation in well Shi23 is 1800 m. The Hongshi depression is characterized by a superimposed deposition of multiple sets of source rocks. The dark mudstone is 800–1410 m in thickness, and two sets of source rocks, E_3^2 and N_1, were primarily developed.

The present analysis of the hydrocarbon generation history revealed that source rocks from the E_3^2 in the Hongshi depression entered the oil generation threshold at a depth of 3800 m in the N_2^1 period (19.0 Ma); the main stage of hydrocarbon expulsion lasted from the N_2^2 period to the N_2^3 period; the hydrocarbon generation stage ended at 4 Ma; currently, hydrocarbon generation has halted. Source rocks from the N_1 entered the oil generation threshold at ~8.53 Ma and are currently in the late hydrocarbon generation stage; due to the formation uplift, hydrocarbon generation became extremely slow after 4 Ma (Fig. 10). Based on the hydrocarbon generation history, we conclude that the deep oil reservoirs had been formed before the late Himalayan movement; tectonic activity destroyed the deep primary oil reservoirs allowing oil and gas migration into late structural traps through
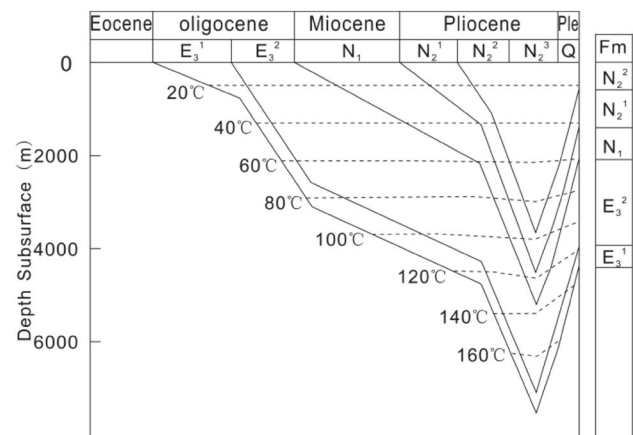

Fig. 9 Source rock burial history in the Shi23 well, Hongshi Depression, Qaidam Basin, China

Fig. 8 Kinetic parameters for products generated from pyrolysis (**a**: kerogen; **b**: source rock) 1 kcal/mol = 4.2 kJ/mol. For comparison, the pre-exponential factor is fixed at $A = 9.9970E + 15$ s^{-1} in all cases
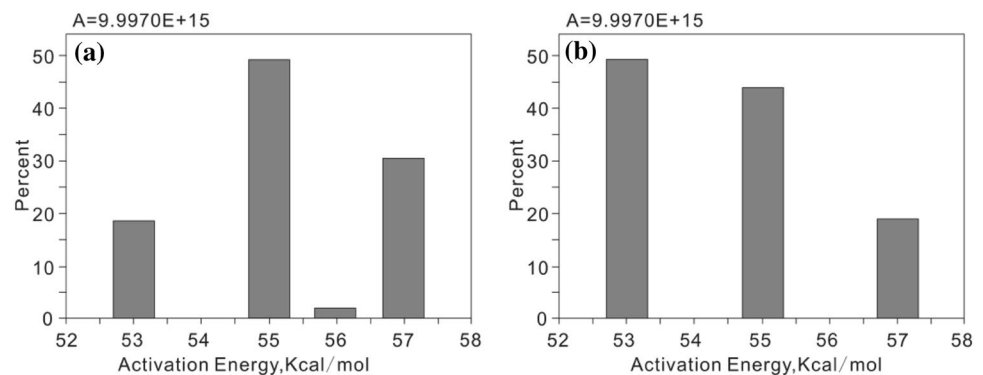
Fig. 10 Hydrocarbon generation history for the source rock and kerogen samples (**a**, E_3^2; **b**, N_1)
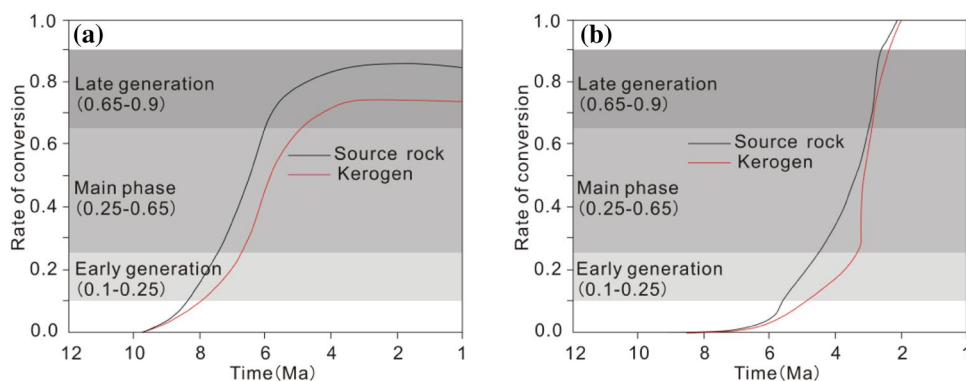
fractures and, thus, forming shallow oil–gas reservoirs in most cases. Exploration practices have confirmed the small scale and low abundance of primary oil reservoirs in the study area, wherein shallow oil reservoirs are generally under the control of fractures and structural traps.

Comparison of the hydrocarbon generation history between the source rock and kerogen samples

A comparison of the hydrocarbon generation history between the source rock and kerogen samples showed that the former entered the hydrocarbon generation threshold earlier than the latter; the difference was significant between the two groups. Furthermore, the source rock sample achieved a significantly higher hydrocarbon generation rate than the kerogen (Fig. 10). Cao et al. (2014) conducted a pyrolysis experiment under the same conditions for the kinetics of hydrocarbon generation from the source rock and kerogen samples in well Lvcan-1 in the Zhahaquan depression, western Qaidam Basin. This group also found that the source rocks entered the oil generation threshold relatively early compared to the kerogen sample; however, the difference was minor and was considered negligible in the previous study. There are differences in the depositional environment between the Hongshi and Zhahaquan depressions. In the Hongshi depression, the gammacerane to C_{30}-hopane ratio as well as the C_{35}-hopane to C_{34}-hopane ratio is greater than 1, indicating high salinity. In the Zhahaquan depression, the gammacerane to C_{30}-hopane ratio ranges between 0.8 and 0.5, whereas the C_{35}-hopane to C_{34}-hopane ratio is between 1 and 0.7. The salinity in the Hongshi depression is significantly higher than that in the Zhahaquan depression. Therefore, we believe that the difference in the time to enter the oil generation threshold between the source rock and kerogen samples is associated with the salinity in the depositional environment of the samples; the higher the salinity, the more significant are the differences. Source rocks from high-salinity depositional environments contain abundant carbonate minerals that may catalyze hydrocarbon generation from organic matter.

Conclusions

Based on the kinetics of hydrocarbon generation, we compared the hydrocarbon generation process of saline lacustrine source rocks and kerogen from the Qaidam Basin using a simulation experiment of pyrolysis in a gold tube-autoclave system. We found that there were large differences in the liquid hydrocarbon yields per unit organic matter between the source rock (690.04 mg/g.TOC) and kerogen samples (278.50 mg/g.TOC). The source rocks had relatively low activation energies and entered the hydrocarbon generation threshold earlier than that of the kerogen samples. The key factor leading to the aforementioned difference could be the catalytic effect of minerals and the presence of soluble organic matter in the source rocks.

Both the source rock and kerogen samples achieved a maximum liquid hydrocarbon yield during the low-mature stage (Easy Ro 0.75%) with 80% of the hydrocarbons being expulsed before the Easy Ro reached 0.8%. Special algal parent materials for hydrocarbon generation in the saline lacustrine basin could be the primary cause leading to the generation of low-maturity oil.

References

Bagri R, Williams PT (2002) Catalytic pyrolysis of polyethy. J Anal Appl Pyrol 63:29–41. https://doi.org/10.1016/S0165 -2370(01)00139-5

Bechar F, Kressmann S, Rudkiewicz JL et al (1992) Experimental simulation in a confined system and kinetics modelling of kerogen and oil cracking. Org Geochem 19(1–3):173–189. https://doi. org/10.1016/0146-6380(92)90035-V

Behar F, Roy S, Jarvie D (2010) Artificial maturation of a typeI kerogen in closed system: mass balances and kinetic modeling. Org Geochem 41:1235–1247. https://doi.org/10.1016/j.orggeochem .2010.08.005

Brooks BT (1948) Active surface catalysts in the formation of petroleum. AAPG Bull 32(12):2269–2286

Cao ZL, Wei ZF, Lin CS et al (2014) The kinetics of oil generation in a Saline Basin: a case study of the source rock of tertiary in Zhahaquan depression, Qaidam Basin, China. Petroleum Sci Technol 32(21):2648–2657. https://doi.org/10.1080/10916466.2014.913623

Connan J (1974) Time-temperature relation in oil genesis: geologic notes. AAPG Bull 58:2516–2521

Fu JM, Shi JY (1975) Theory and practice about petroleum evolvement (I): theory and stages of petroleum evolvement. Geochimica 4(2):87–110 **(in Chinese)**

Guo XL, Xiong M, Zhou Q et al (2009) Petroleum generation and expulsion kinetics: a case study of the sahejie formation source rocks from Linnan Sag of Huimin depression. Acta Sedimentol Sinica 27(4):723–731 **(in Chinese)**

Guo ZQ, Ma YS, Lin WH et al (2017) Main factors controlling the formation of basement hydrocarbon reservoirs in the Qaidam Basin, western China. J Petrol Sci Eng 149:244–255. https://doi.org/10.1016/j.petrol.2016.10.029

Hanson AD, Ritts BD, Zinniker D et al (2001) Upper Oligocene lacustrine source rocks and petroleum systems of the northern Qaidam Basin, northwest China. AAPG Bull 85:601–620

Huang DF, Li JC, Zhou ZH et al (1984) Evolvement and mechanism of hydrocarbon generation from continental organic matters. Petroleum Industry Press, Beijing, pp 171–179

Huang CG, Zhao F, Yuan JY et al (2016) The characteristics of dolomite reservoir in saline lacustrine Basin, Qaidam, China. Carbonates Evaporites 31:307–317. https://doi.org/10.1007/s13146-015-0267-0

Jiang QG, Wang YB, Jz Qin (2010) Kinetics of the hydrocarbon generation process of marine source rocks in South China. Petrol Explor Dev 37(2):174–180. https://doi.org/10.1016/s1876-3804(10)60024-9

Lewan MD, Winters JC, Mcdonald JH (1979) Generation of oil-like pyrolyzates from organic-rich shales. Science 203:897–899. https://doi.org/10.1126/science.203.4383.897

Li SY, Lin SJ, Guo SH et al (2002) Catlaytic effects of minerals onhydrocarbon generation in kerogen degradation. J Univ Petrol China 26(1):69–74. https://doi.org/10.3321/j.issn:1000-5870.2002.01.022 **(in Chinese)**

Li E, Pan CC, Yu S et al (2013) Hydrocarbon generation from coal, extracted coal and bitumen rich coal in confined pyrolysis experiments. Org Geochem 64:58–75. https://doi.org/10.1016/j.orggeochem.2013.09.004

Liu JZ, Tang YC (1998) An example for predicting methane generation by kerogen kinetic experiment. Chin Sci Bull 43:1187–1191 **(in Chinese)**

Liu Y, He K, Li XQ et al (2016) Hydrocarbon generation kinetics and the efficiency of petroleum expulsion of lacustrine source rocks: taking the Qingshankou formation in the Songliao Basin as an example. Geoscience 30(3):627–634. https://doi.org/10.3969/j.issn.1000-8527.2016.03.013 **(in Chinese)**

Ma ZL, Zheng LJ, Li ZM (2013) The effect of salts on hydrocarbon generation and expulsion of argillaceous source rock. J Southwest Petrol Univ (Sci Technol Ed) 35(1):43–51. https://doi.org/10.3863/j.issn.1674-5086.2013.01.006 **(in Chinese)**

Mackenzie AS, Li RW, Maxwell JR et al (1983) Molecular measurements of thermal maturation of cretaceous shale from the overthrusbelf. Adv Org Geochem, Wyoming, pp 496–503

Pan CC, Jiang LL, Liu JZ et al (2010) The effects of calcite and montmorillonite on oil cracking in confined pyrolysis experiments.

Org Geochem 41:611–626. https://doi.org/10.1016/j.orggeochem.2010.04.011

Peng DH (2005) Evolutionary process of hydrocarbon generation and characteristics of source rocks of the tertiary salt lacustrine facies in the west of Qaidam Basin. Dissertation, Guangzhou institute of geochemistry, Chinese Academy of Science, pp 92–101 **(in Chinese)**

Reynolds JG, Burnham AK (1995) Comparison of kinetic analysis of source rocks and kerogen concentrates. Org Geochem 23(1):11–19. https://doi.org/10.1016/0146-6380(94)00114-G

Saxby JD, Chatfield P, Taylor GH et al (1992) Effect of clay minerals on products from coal maturation. Org Geochem 18(3):373–383. https://doi.org/10.1016/0146-6380(92)90078-C

Seewald JS, Benitez-Nelson BC, Whelan JK (1998) Laboratory and theoretical constraints on the generation and composition of natural gas. Geochim Cosmochim Acta 62(9):1599–1617. https://doi.org/10.1016/S0016-7037(98)00000-3

Song YT, Li SQ (1995) Experimental study on simulating hydrocarbon generation of coccolithophoridaes by heating: I. Generation rate and property of hydrocarbons, characteristic of alkanes and alkenes. Geol J Univ 1(2):95–106

Sweeney JJ, Burnham AK (1990) Evaluation of a simple model of vitrinite reflectance based on chemical kinetics. Am Asso Petrol Geol Bull 74:1559–1570

Tang QY, Zhang MJ, Zhang TW (2014) Kinetic pyrolysis simulation of hydrocarbon generation in shale system: a case study on pearl river mouth Basin, China. Geochimica 43(5):518–528 **(in Chinese)**

Tannenbaum E, Kaplan IR (1985) Role of minerals in the thermal alteration of organic matter. I-generation of gases and condensates under dry condition. Geochim Cosmochim Acta 49(12):2589–2604. https://doi.org/10.1016/0016-7037(85)90128-0

Tissot BP, Espitalié J (1975) L' évolution de la matièreorganique des sédiments: application d'une simulation mathématique. Revue de l'Institut Français du Pétrole 30:743–777. https://doi.org/10.2516/ogst:1975026

Tissot BP, Pelet R, Ungerer P (1987) Thermal history of sedimentary basins, maturation indices, and kinetics of oil and gas generation. AAPG Bull 71(12):1445–1466

Wang J, Jin Q, Ma GZ et al (2009) Catalytic action of sulphate evaporates in pyrolytic gas generation of source rocks. Nat Gas Geosci 20(1):26–31 **(in Chinese)**

Waples D (1981) Time and temperature in petroleum formation: application of lopatin's method to petroleum exploration. AAPG Bull 64(6):916–926

Xiao XM, Zeng QH, Tian H et al (2005) Origin and accumulation model of the AK-1 natural gas pool from the Tarim Basin, China. Org Geochem 36:1285–1298. https://doi.org/10.1016/j.orggeochem.2005.04.001

Xie QL, Zhou ZY, Lu MY (2000) Organic matter enclosed in carbonate minerals-a kind of important hydrocarbon-producing matter. Acta mineralogicasinica 20(1):59–62. https://doi.org/10.3321/j.issn:1000-4734.2000.01.011 **(in Chinese)**

Zhang ZL, Ren YH, Yan ZL et al (2005) Kinetics on hydrocarbon generation from fatty acid ester in the presence of natural minerals at low temperature. Geochimica 34(3):263–268. https://doi.org/10.3321/j.issn:1000-5870.2005.05.024 **(in Chinese)**

Zhou FY, Peng DH, Bian LZ (2002) Progress in the organic matter study of immature oils in the Qaidam Basin. Acta Geol Sinica 76(1):107–113. https://doi.org/10.3321/j.issn:0001-5717.2002.01.014 **(in Chinese)**